Click chemistry–enabled CRISPR screening reveals GSK3 as a regulator of PLD signaling

Timothy W. Bumpus[a], Shiying Huang[a], Reika Tei[a], and Jeremy M. Baskin[a,1]

[a]Department of Chemistry and Chemical Biology and Weill Institute for Cell and Molecular Biology, Cornell University, Ithaca, NY 14853

Edited by Jennifer A. Doudna, University of California, Berkeley, CA, and approved October 25, 2021 (received for review December 8, 2020)

Enzymes that produce second messengers are highly regulated. Revealing the mechanisms underlying such regulation is critical to understanding both how cells achieve specific signaling outcomes and return to homeostasis following a particular stimulus. Pooled genome-wide CRISPR screens are powerful unbiased approaches to elucidate regulatory networks, their principal limitation being the choice of phenotype selection. Here, we merge advances in bioorthogonal fluorescent labeling and CRISPR screening technologies to discover regulators of phospholipase D (PLD) signaling, which generates the potent lipid second messenger phosphatidic acid. Our results reveal glycogen synthase kinase 3 as a positive regulator of protein kinase C and PLD signaling. More generally, this work demonstrates how bioorthogonal, activity-based fluorescent tagging can expand the power of CRISPR screening to uncover mechanisms regulating specific enzyme-driven signaling pathways in mammalian cells.

phospholipase D | click chemistry | CRISPR screening | GSK3 | CRISPRi

Cells rely on carefully regulated signaling cascades to integrate and respond to information from their surrounding environment (1). Key components of these pathways are the enzymes that generate second messengers. Because of the potency of second messengers, the enzymes that produce them are highly regulated, and revealing the mechanisms underlying such regulation is critical to understanding both how cells achieve specificity of signaling outcomes and a return to homeostasis following stimulation (2).

Phospholipase D (PLD) enzymes exemplify this paradigm. Several cell-surface receptors and intracellular proteins stimulate PLDs to produce the pleiotropic lipid second messenger phosphatidic acid (PA) (3, 4). PLD/PA signaling controls many cellular processes, including cytoskeletal organization, membrane trafficking dynamics, and growth and proliferative pathways. Given the potency of PA signaling, its dysregulation has major consequences. Hyperactive PLD signaling is a hallmark of several cancers and autoimmune and neurodegenerative diseases (5, 6), whereas a loss of PLD function in mice causes deficits in learning and memory (7). Thus, understanding the mechanisms underlying the regulation of PLD signaling is of utmost importance. Indeed, PLD enzymes are subject to a high degree of regulation; yet, it remains unclear how PLDs integrate input from a diverse collection of regulatory proteins to ensure appropriate levels of agonist-induced signaling events within a desired homeostatic range. To reveal these connections and understand how they fit into larger regulatory networks, we set out to identify additional uncharacterized factors that affect the strength of PLD signaling.

Unbiased genome-wide loss-of-function screens are powerful approaches to identify new regulators of physiological processes. In particular, CRISPR-Cas9–based genome-wide pooled screening techniques have democratized this strategy for use in mammalian cells because of their excellent genomic coverage, relatively low cost, and ease of implementation and data analysis (8–10). In a typical experiment, a pooled lentiviral library is generated, containing several single guide RNAs (sgRNAs) per gene, and a large population of cells expressing Cas9 or an engineered variant [e.g., for CRISPR interference, or CRISPRi, a fusion of catalytically dead Cas9 and the transcriptional repressor KRAB (11)] is infected such that each cell receives a single sgRNA. Critically, subsets of cells are then selected for a desired phenotype, and the identity of enriched genes that modulate the phenotype are identified in the selected population by next-generation sequencing of the sgRNAs targeting those genes. The power, but also a main limitation, of these approaches stems from the care and creativity that goes into design of the selection step for enriching cells with a desired phenotype. Typically, selection involves either survival in the face of a cytotoxic challenge (8, 9) or enrichment by fluorescence-activated cell sorting (FACS) based on changes in cellular fluorescence (12, 13).

For CRISPR-Cas9–based genome-wide screening, the most commonly used fluorescent-labeling methods include expression of fluorescent protein reporter constructs (12) or antibody labeling (13). Though unquestionably powerful, these approaches are limited in the scope of what they can report on: changes in gene expression and abundance of particular epitopes targetable by antibodies. Yet, the universe of selective fluorescent labeling tools is much wider. The chemical biology community has developed a diverse collection of labeling strategies that enable selective fluorescent tagging or visualization of target biomolecules within living cells (14). These include metabolic labeling with bioorthogonal reporters (15–17), activity-based tagging of enzymes (18), and activity-based sensing tools (19). Collectively, these approaches can visualize targets as diverse as glycans, lipids, metabolites, and ions, including many potent second messengers as well as proteins

Significance

The application of CRISPR-Cas9 to genome-wide screening has revolutionized our ability to discover new functions for genes and regulators of physiological processes. However, a major constraint placed on such screens is the choice of phenotypic selection step, typically limited to live/dead or conventional fluorescent reporter/labeling. Here, we develop a CRISPR interference–based screening platform harnessing click chemistry tagging to reveal regulators of a specific signaling pathway. Using this tool, we discovered a regulatory circuit involving glycogen synthase kinase 3 and protein kinase C in the control of phospholipase D signaling. More broadly, this work illustrates how emergent chemical biology approaches can expand the power of genome-wide CRISPR screening to elucidate mechanisms regulating specific enzyme-driven signaling pathways.

Author contributions: T.W.B., S.H., R.T., and J.M.B. designed research; T.W.B., S.H., and R.T. performed research; T.W.B., S.H., R.T., and J.M.B. analyzed data; and T.W.B. and J.M.B. wrote the paper.

The authors declare no competing interest.

This article is a PNAS Direct Submission.

[1]To whom correspondence may be addressed. Email: jeremy.baskin@cornell.edu.

This article contains supporting information online at http://www.pnas.org/lookup/suppl/doi:10.1073/pnas.2025265118/-/DCSupplemental.

Published November 22, 2021.

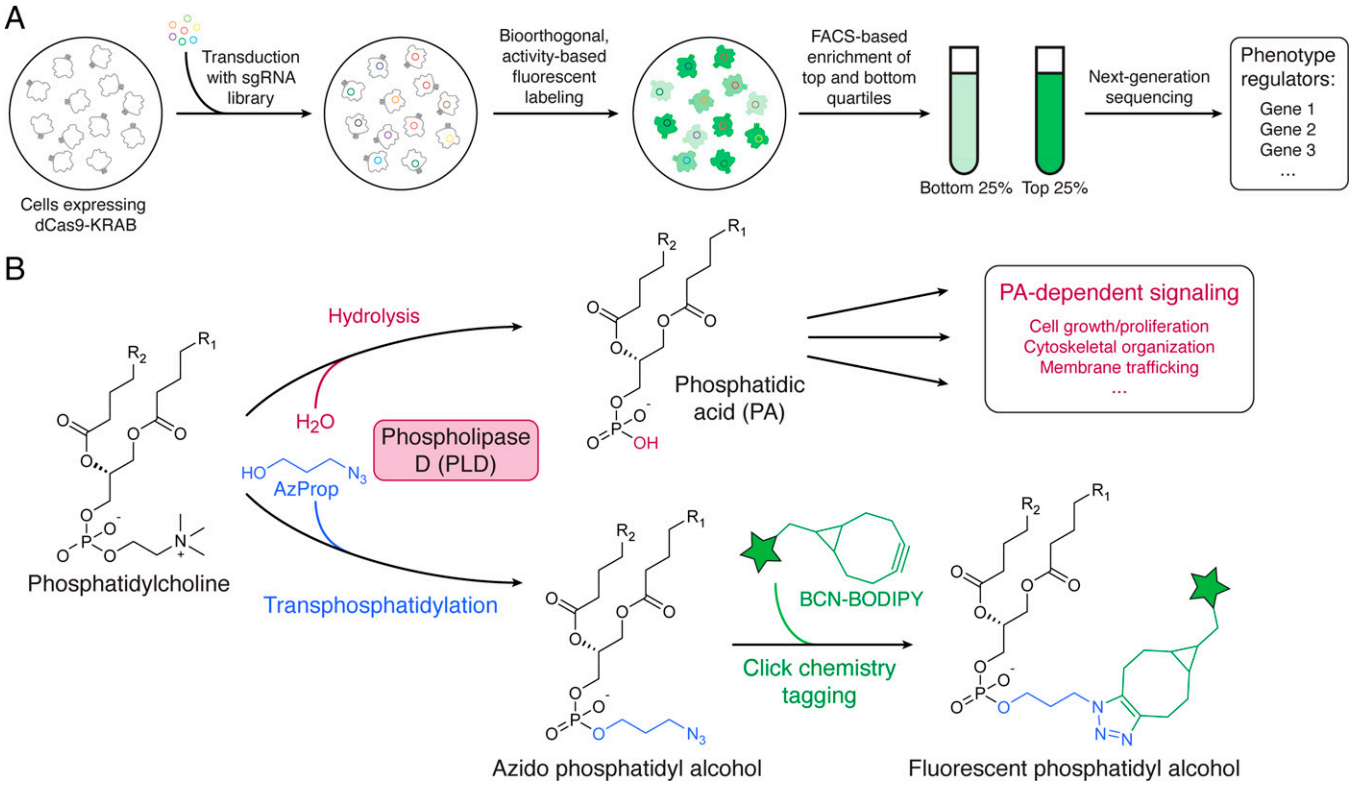

Fig. 1. Combining pooled CRISPRi screening with bioorthogonal labeling to visualize phospholipase D signaling. (*A*) Scheme for pooled CRISPR screening based on bioorthogonal labeling to uncover regulators of the pathway of interest targeted by the bioorthogonal labeling step. (*B*) PLD-mediated PA synthesis and IMPACT method for detecting PLD activity. Top arrow: PLD signaling involves hydrolysis of phosphatidylcholine to generate the lipid second messenger PA. Bottom arrow: IMPACT as a means to generate fluorescent reporters of PLD signaling. IMPACT takes advantage of PLD-catalyzed transphosphatidylation with 3-azidopropanol followed by click chemistry tagging via strain-promoted azide-alkyne cycloaddition with a fluorescent cyclooctyne reagent (BCN-BODIPY) to generate fluorescent phosphatidyl alcohol reporters to enable FACS-based enrichment of cells based on their PLD activity.

and nucleic acids. These small molecule reporter strategies are therefore ripe for combination with pooled CRISPR screens to expand the phenotypes that this powerful forward-genetic approach can address (Fig. 1*A*). Indeed, examples of their use in probing processes including glycan biosynthesis (20), lysosomal pH (21), and redox balance (22) have revealed new regulators of these processes.

In the arena of PLD signaling, we have developed an activity-based imaging method that fluorescently tags intracellular membranes bearing endogenous PLD activity with fluorescent reporter lipids. The method, termed imaging phospholipase D activity with clickable alcohols via transphosphatidylation (IMPACT), takes advantage of a promiscuous enzymatic activity of PLDs (23). These enzymes physiologically hydrolyze phosphatidylcholine (PC) to make PA (Fig. 1*B*), but they will also catalyze transphosphatidylation with exogenously supplied primary alcohols to produce phosphatidyl alcohol lipids (4). By using clickable primary alcohols for the transphosphatidylation step and subsequent bioorthogonal click chemistry tagging, IMPACT generates fluorescent phosphatidyl alcohols that are reporters of endogenous PLD activity within live cells (23–27) (Fig. 1*B*). Because IMPACT serves as a single-cell fluorescent label for the extent of PLD signaling (23), we reasoned that it could serve as the basis of selection in a genome-wide CRISPR-Cas9 screen to identify new regulators of PLD signaling.

In this study, we develop such an IMPACT-based CRISPR screening approach that uses pooled genome-wide CRISPR-Cas9 screening, with IMPACT labeling–dependent FACS-based enrichment as the selection step, to identify new factors that modulate the strength of PLD signaling (Fig. 2*A*). As a test case for this approach, we applied this method to interrogate regulation of the protein kinase C (PKC)–PLD signaling axis. PKCs, one of the most potent and well-characterized stimulators of PLD signaling, act by recruiting the PLD1 isozyme to the plasma membrane and activating its production of PA (4, 28). Several factors that stimulate PKC–PLD signaling are well established, but how cells modulate the levels or activity of these enzymes to ensure homeostasis rather than uncontrolled signaling remains poorly understood. To reveal regulatory mechanisms, we performed an IMPACT-based screen wherein we stimulated PKC–PLD signaling and identified genes whose inactivation by CRISPRi led to either enhancement or suppression of PLD signaling as read out by IMPACT. From this screen, we identified and characterized glycogen synthase kinase 3 (GSK3) as an activator of PLD signaling. Our results reveal a putative regulatory circuit involving GSK3, PKC, and PLD that would enable cells to both be primed for potent agonist signaling and subsequently return to homeostasis.

Results

Among the several CRISPR platforms amenable to genome-wide screening, we chose to use CRISPRi (9, 11). This methodology, featuring endonuclease-dead Cas9 fused to the transcriptional repressor KRAB, results in a functional equivalent to gene knockdown. Similar to conventional CRISPR knockout, CRISPRi is scalable to the whole-genome level, but it has added benefits, including greater coverage because of improved survival from knockdown versus knockout of certain essential genes and elimination of potential complications deriving from long-range effects of double-strand breaks (29).

We first generated a lentiviral sgRNA library, using a human genome-wide CRISPRi-v2–pooled library (30) containing five

sgRNAs targeting each gene in human embryonic kidney (HEK) 293TN cells. We then transduced a K562 cell line stably expressing the dCas9-KRAB fusion (K562i cells) with the sgRNA lentiviral library at a multiplicity of infection (MOI) of ∼0.4 to ensure that each cell would receive no more than one sgRNA on a large scale (∼125 million cells, or ∼1,000× coverage for the sgRNA library). Following puromycin selection, PKC–PLD signaling was stimulated by the addition of phorbol-12-myristate-13-acetate (PMA), and IMPACT was performed by the addition of 3-azidopropan-1-ol for 20 min followed by a rinse and strain-promoted azide-alkyne cycloaddition tagging with a bicyclononyne-BODIPY fluorophore (BCN-BODIPY) (31). To ensure the stability of cellular fluorescence over subsequent hours of sorting, cells were then fixed with formaldehyde. A small aliquot of the labeled cells was reserved, and the remainder was subjected to FACS, with the top and bottom quartiles of the IMPACT-labeled population being collected (32). Following DNA extraction and sgRNA amplification, the sgRNA identity and abundance in each population was determined by Illumina next-generation sequencing (Fig. 2*A*).

By comparing sgRNA enrichment in the top and bottom quartiles relative to either each other or to the unsorted population (30), we identified 160 genes whose perturbation by CRISPRi had a significant effect on the level of IMPACT labeling (Fig. 2*B* and *SI Appendix*, Table S1). We designated the 81 genes whose sgRNAs were enriched in either the 1) unsorted

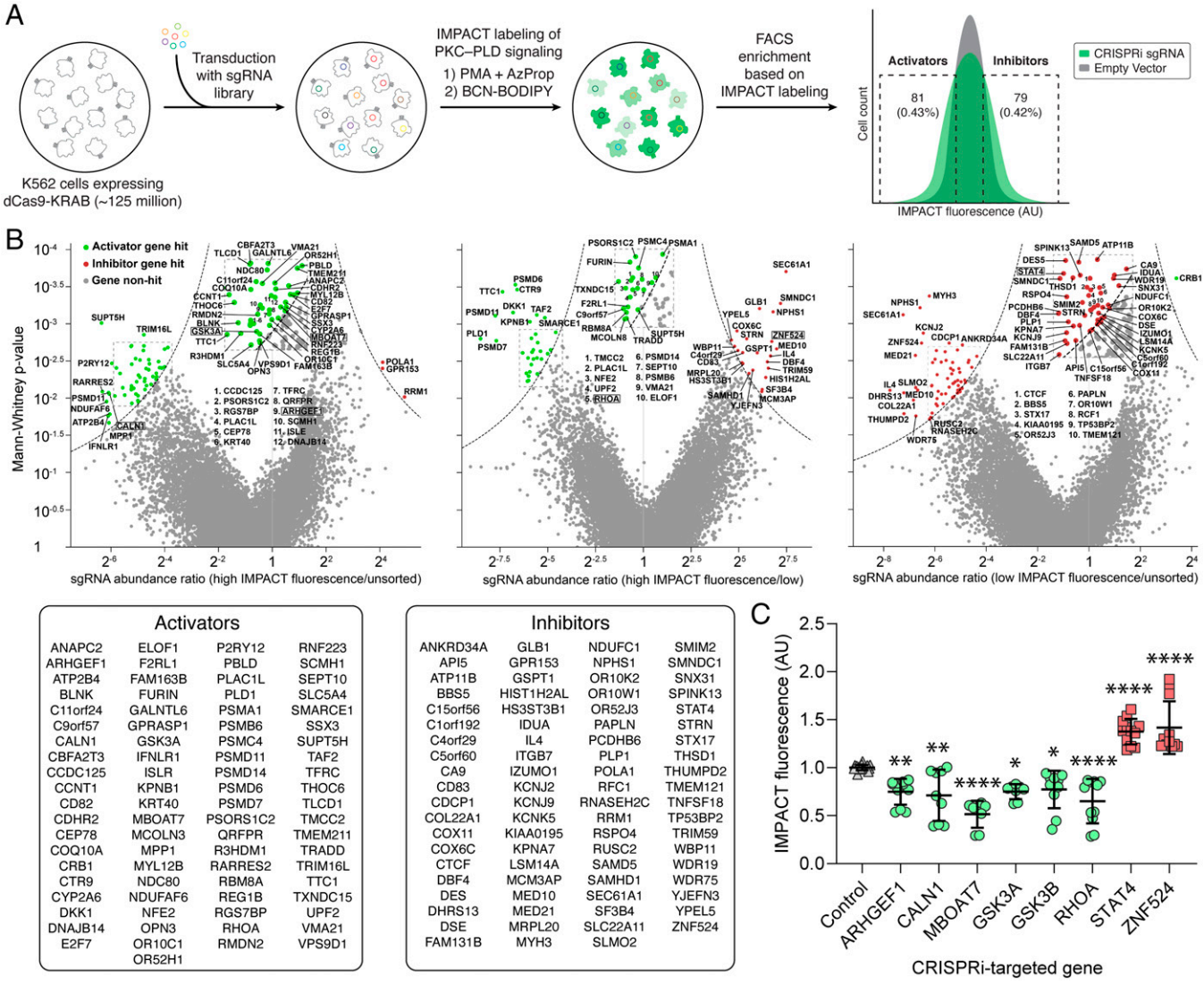

Fig. 2. Combining IMPACT with genome-wide CRISPRi screening to identify regulators of protein kinase C–PLD signaling. (*A*) Experimental overview. A population of ∼125 million K562-dCas9-KRAB (K562i) cells was transduced at an MOI of ∼0.4 with a lentiviral sgRNA library of sgRNAs targeting the entire human genome. PKC-mediated PLD signaling was then stimulated by the addition of PMA, and IMPACT labeling was performed to fluorescently label cells according to PLD signaling activity. The top and bottom quartiles of the labeled population were collected via FACS, and enriched sgRNAs in those populations were identified by Illumina next-generation sequencing. (*B*) Results from the screen. Volcano plots depict the three pairwise comparisons of sgRNA levels in high IMPACT, low IMPACT, and unsorted cell populations. *X*-axes show ratio of sgRNA abundance in the indicated populations, *y*-axes show the Mann–Whitney *U* test *P* value. (*Insets*) Boxed region, enlarged for clarity. Green data points: genes predicted to be "activators" of PLD; red data points: genes predicted to be "inhibitors" of PLD. Shown below is a combined listing of all putative activators and inhibitors from the screen. See *SI Appendix*, Table S1 for separate lists of hits from each pairwise comparison (i.e., from each volcano plot). (*C*) Validation of several putative regulators of PLD signaling. K562i cells expressing CRISPRi sgRNA targeting the indicated gene (shown in boxes in volcano plot) were labeled by IMPACT with PMA stimulation, and flow cytometry analysis was performed. Plotted are the mean fluorescence intensities of the labeled populations, with background fluorescence subtracted and normalized to control sgRNA (gray). $n = 8$ to 21, ANOVA (Tukey) $^*P < 0.05$; $^{**}P < 0.01$, $^{****}P < 0.001$.

relative to high IMPACT, 2) low IMPACT relative to high IMPACT, or 3) low IMPACT relative to unsorted populations as "activators" of PKC–PLD signaling because their CRISPRi-mediated knockdown resulted in lower levels of IMPACT labeling (Fig. 2*B*, green data points). Correspondingly, we denoted the 79 enriched in either 1) high IMPACT relative to unsorted, 2) high IMPACT relative to low IMPACT, or 3) unsorted relative to low IMPACT populations as "inhibitors" of PKC–PLD signaling (Fig. 2*B*, red data points).

Gratifyingly, among the enriched activators was PLD1, the mammalian PLD isozyme most strongly stimulated by PMA (4, 23). The identification of the Rho family GTPase RhoA and the guanine nucleotide exchange factor (GEF) ARHGEF1 as activators in the screen serves as a further validation of the results. RhoA is a well-characterized activator of PLDs that works in concert with PKC (33), and ARHGEF1 is a GEF for RhoA that drives it to the active, GTP-bound form (34–36). Interestingly, among the hits were BBS5 (37), C1orf192 (38), and WDR19 (39), all of which are related to cilia, a structure whose physiological function requires the regulated transport of PLD by the BBSome complex (40–42). Though we did not identify any PKCs as activators, there are many PKC isoforms with overlapping functions (4, 28, 43); consequently, knockdown of any single isoform could be compensated by the activities of other isoforms in the presence of the strong PMA stimulus.

To validate the generality of the screen, we generated stable cell lines expressing CRISPRi sgRNAs targeting nine genes encompassing predicted activators and inhibitors from all three volcano plots. CRISPRi knockdown of five predicted activators (ARHGEF1, CALN1, MBOAT7, GSK3A, and RHOA) led to a decrease in IMPACT fluorescence as quantified by flow cytometry (Fig. 2*C*). Similarly, CRISPRi knockdown of two predicted inhibitors, STAT4 and ZNF524, led to increases in cellular IMPACT fluorescence (Fig. 2*C*). Two additional predicted inhibitors, API5 and RUSC2, did not affect IMPACT fluorescence. By examining all three pairwise comparisons between the three populations (i.e., high IMPACT, low IMPACT, and unsorted cells), we were able to capture a larger number of potential hits, and indeed, hits were validated from all three volcano plots. Yet, we note potential confounding factors, for example, sick/dead cells or doublets absent from sorted populations but potentially present in the unsorted population, which highlights the importance of secondary validation of any putative hit from such a screen.

Interestingly, among the activators of IMPACT labeling was glycogen synthase kinase 3α (GSK3α). GSK3α and its close paralog GSK3β are major Ser/Thr kinases that regulate diverse processes including metabolism, proliferation, apoptosis, and signaling, and they have been extensively explored as therapeutic targets in many diseases (44). Because of the central role of GSK3 in cell signaling, we hypothesized that understanding how GSK3 affects PLD signaling would reveal general principles of how cells regulate PLD signaling in the context of other signaling pathways.

First, as described above (by generation of stable CRISPRi cell lines), we confirmed the finding from the high-throughput screen by demonstrating that CRISPRi knockdown of either GSK3A or its close paralog GSK3B resulted in lower levels of PMA-stimulated PLD activity using IMPACT labeling followed by flow cytometry analysis (Fig. 2*C*). We then perturbed GSK3 using alternative, pharmacological means and assessed cellular PLD activity using IMPACT. For these studies, we used either MDA-MB-231 cells, an aggressive breast cancer cell line with high PLD activity, or the K562i cell line used for the genome-wide CRISPRi screen (45). The cells were treated with LY2090314 (46), an inhibitor of both GSK3 isoforms, or vehicle for 24 h, mimicking the sustained GSK3 loss of function achieved by CRISPRi knockdown. We found that LY2090314 treatment led to a substantial decrease (~50 to 60%) in the extent of PMA-stimulated IMPACT labeling as quantified by high-performance liquid chromatography (HPLC) analysis of fluorescent phosphatidyl alcohols generated by IMPACT in cells receiving LY2090314 compared to control (Fig. 3*A*).

As an alternative to IMPACT readout of PLD activity, we found that LY2090314 treatment of K562i cells decreased PLD activity using the traditional butanol transphosphatidylation assay (47) with quantification of phosphatidyl butanol by liquid chromatography–mass spectrometry (*SI Appendix*, Fig. S1). To further support these results, we demonstrated that overnight treatment of MDA-MB-231 cells with two additional pan-GSK3 inhibitors caused a similar decrease in IMPACT labeling (*SI Appendix*, Fig. S2). Isoform-selective inhibitors (48) revealed partial contributions from both GSK3A and GSK3B to this phenotype (*SI Appendix*, Fig. S2). Finally, we verified that the treatment with GSK3 inhibitors did not affect cell viability (*SI Appendix*, Fig. S3). We next set out to establish a mechanism for how GSK3 regulates PLD signaling.

Among the many established signaling roles for GSK3 is as a negative regulator of Wnt/β-catenin signaling (49). Here, GSK3 phosphorylation of β-catenin promotes its degradation, suppressing the expression of Wnt target genes that govern proliferation and other cellular responses (50). If the mechanism by which GSK3 affects PLD signaling occurs via its role in the Wnt/β-catenin pathway, we would predict that Wnt activation in a physiological manner by stimulation with Wnt ligands would also diminish IMPACT labeling. To test this hypothesis, we treated cells with conditioned media from Wnt3a-producing or control cells and quantified levels of IMPACT-derived lipids. Surprisingly, we found that treatment with Wnt3a had no effect on the cells' ability to produce IMPACT-derived phosphatidyl alcohols, indicating that in this context, the modulation of PLD activity by GSK3 occurs via an alternate means (44, 49, 51) (*SI Appendix*, Fig. S4).

We then aimed to identify whether GSK3 acts directly on PLD to acutely modulate its activity or whether the effect of GSK3 on PLD signaling requires a longer timescale. Thus, we varied the duration of LY2090314 treatment and found that, in contrast to treatment for 24 h, exposure of cells to LY2090314 for 1 or 2 h had no effect on the extent of IMPACT labeling (Fig. 3*B*). The requirement for an extended time of GSK3 inhibition to have effects on PLD activity suggested that, rather than directly regulating PLD signaling via phosphorylation of PLDs, GSK3 might regulate the production and/or levels of PLD proteins (44).

We next sought to distinguish whether GSK3 inhibition affected cellular levels of PLDs. We found that MDA-MB-231 cells treated with LY2090314 for 24 h led to lower levels of PLD1 and PLD2, the two major PLD isozymes responsible for PA generation by PC hydrolysis (Fig. 3*C*). Interestingly, the magnitude of the protein reduction was smaller than the reduction in IMPACT labeling, suggesting additional effects of LY2090314 might affect PLD activity (Fig. 3*A*). Because we were using a PKC stimulus (PMA) to activate PLD signaling in these experiments, we also assessed the levels of PKCα, a major PKC isoform responsible for PLD activation in response to PMA (4, 52), and found that LY2090314 treatment also led to a similar reduction in protein levels of PKCα (Fig. 3*C*).

GSK3 can regulate both transcription and protein degradation, both of which would affect the overall levels of its targets (44). Because of the impracticality of blocking protein degradation pathways for 24 h, we instead tested whether inhibition of GSK3 affected the messenger RNA levels of PLD and PKC as a way to assess the effects of GSK3 on transcription. Using qRT-PCR analysis, we found that LY2090314 treatment of MDA-MB-231 cells led to decreases in transcript levels for the major splice forms of PLD1 (53, 54) and PLD2 (55) as well as

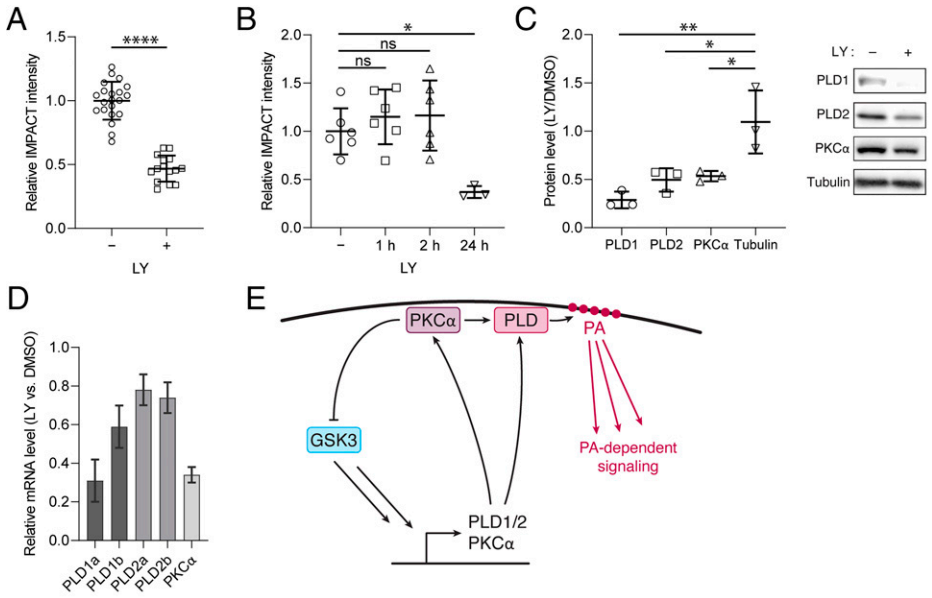

Fig. 3. GSK3 regulates PA-dependent signaling via the expression of PLD and PKC. (*A* and *B*) MDA-MB-231 cells were treated with the GSK3 inhibitor LY2090314 (20 nM, blue) or vehicle (dimethyl sulfoxide [DMSO], black) for the indicated length of time and then subjected to IMPACT labeling by the addition of 3-azidopropanol (1 mM) and PMA (100 nM), rinsing, and strain-promoted azide-alkyne cycloaddition tagging with BCN-BODIPY. Lipid extracts were generated, and the IMPACT-derived fluorescent lipids were detected and quantified using fluorescence-coupled HPLC. (*C*) MDA-MB-231 cells were treated with LY2090314 (20 nM) or DMSO vehicle for 24 h. Protein lysates were collected, analyzed, and quantified via Western blot. (*D*) MDA-MB-231 cells were treated with LY2090314 (20 nM) or DMSO vehicle for 24 h. Cellular messenger RNA was collected, converted to complementary DNA via reverse transcription, and quantified via qPCR. ΔΔCp values were calculated by comparison to a tubulin control. Plotted are relative messenger RNA levels ($2^{-\Delta\Delta Cp}$) for each transcript of interest in cells treated with LY2090314 as compared to those treated with DMSO vehicle. (*E*) Model for how GSK3 activity promotes the transcription of PKCα and PLD1/2, causing their levels to increase and priming cells to have elevated agonist-induced PKC–PLD-mediated PA production and signaling. To attenuate PA synthesis and maintain homeostasis, an effect of PKC activation is its phosphorylation and inactivation of GSK3, thus reducing the transcription of PKC and PLD to reset the system. Statistical analysis: (*A*) $n = 14$, $^{****}P = 1.5 \times 10^{-14}$, Student's *t* test. (*B* and *C*) $n = 6$ (*B*) and $n = 3$ (*C*), ANOVA with post hoc Tukey test; $^{*}P < 0.05$; $^{**}P < 0.01$; $^{****}P < 0.0001$; ns, not significant. (*D*) $n = 6$. Error bars: 1σ shown around the mean in *A*–*C* and 95% CI in *D*.

PKCα (Fig. 3*D*). On the basis of these data, we propose that GSK3 acts as an activator of PKC–PLD signaling by enhancing de novo production of PLD and PKC enzymes. As discussed in detail in *Discussion*, these data support a model wherein this GSK3-mediated elevation of PLD and PKC synergistically primes cells for agonist-stimulated PKC–PLD-mediated PA signaling and also allows for a return to homeostatic levels following the PKC-mediated down-regulation of GSK3 activity (56) (Fig. 3*E*).

Discussion

In this study, we have merged two complementary emerging toolsets to reveal insights into the regulation of cell signaling pathways. CRISPR screening using IMPACT harnesses the accessibility and power of whole-genome, forward-genetic screens afforded by pooled CRISPRi platforms (9, 30) and the selectivity of IMPACT, an activity-based, bioorthogonal-labeling strategy that fluorescently tags cellular membranes according to their levels of PLD signaling (23). By performing such a screen with PLD stimulation by PMA, we revealed many factors as potential regulators of PKC-dependent PLD signaling. Among these candidates, we characterized GSK3 as a positive regulator of PKC–PLD signaling.

We can draw several conclusions from this work. First, regarding the mechanism by which GSK3 regulates PKC–PLD signaling, GSK3 inhibition led to comparatively smaller decreases in PLD and PKC levels. Yet, because IMPACT is a readout of PLD activity, not levels, of PLDs, the combination of these reductions in protein levels accounts for the larger overall reduction in IMPACT labeling observed by GSK3 inhibition. Because PLD activity, and thus IMPACT labeling, requires the presence of both proteins simultaneously in a protein–protein interaction (52, 57), the overall activity of the system is reasonably approximated as the product of the two protein levels, bringing the reduction in protein levels (to ∼60 to 70% of control in each case) and the reduction in IMPACT labeling (∼40 to 50% of control) into good alignment. The synergistic effect of GSK3 on the production of PLD and PKC suggests a role for GSK3 as a central regulator of the PKC–PLD signaling cascade that occurs downstream of phospholipase C pathways emanating from the activation of various cell-surface receptors (4, 58).

Second, our discovery of GSK3 as a positive regulator of PKC–PLD signaling points to a potential self-regulating circuit involving these signaling proteins. GSK3 is, itself, highly regulated, and a major mechanism for such regulation is inhibitory phosphorylation by other kinases at N-terminal Ser residues (Ser9 in GSK3α and Ser21 in GSK3β) (44, 59). Among the phosphorylation targets of PKC is the N-terminal Ser residues of GSK3, which causes a downregulation of GSK3 activity (56). These reciprocal connections between PKC and GSK3—GSK3 enhances PKC levels and PKC downregulates GSK3 activity—would thus provide the cell with the ability to sense and regulate PKC–PLD signaling activity. In this model, PKC and PLD levels are sustained in part via GSK3 activity, which induces the transcription of these genes (Fig. 3*E*). The resultant elevation of PKC and PLD protein levels primes cells for productive PKC and PLD signaling, either at a tonic level or when acutely stimulated by upstream generation of appropriate signals. One effect of elevated PKC–PLD signaling is the PKC-mediated phosphorylation of GSK3 (56), which would attenuate PKC and PLD transcription, causing a reduction of PKC and PLD

protein levels. Thus, this balancing of the levels and activity of GSK3 and PKC allows the cell to modulate levels of PLD-dependent PA signaling within a desired physiological range. Interesting future directions will include elucidating the relevant effects of GSK3 on the gene regulatory machinery (44, 60) to achieve this outcome.

Finally, this first IMPACT-based CRISPRi screen with PMA establishes the utility of this approach for revealing regulators of PLD signaling. PLD enzymes are integrators of many different types of inputs (3, 4, 27), and we envision similar screens using alternate PLD stimuli, including agonists of specific G protein-coupled receptors, receptor tyrosine kinases, or integrins, as a means to elucidate new mechanisms that regulate PLD signaling. More broadly, our work demonstrates how a bioorthogonal metabolic labeling tool can enable a FACS-based pooled CRISPR screen to reveal regulators of a specific metabolic pathway, in this case the PLD-mediated conversion of PC to PA. Given the wide array of bioorthogonal metabolic labeling methods for fluorescently tagging glycans (17), lipids (61), protein posttranslational modifications (16), and other cellular metabolites as well as fluorescent activity-based profiling (18) and sensing probes (19), we envision that the IMPACT–CRISPRi paradigm will inspire development of complementary bioorthogonal tagging–enabled CRISPR screening approaches to elucidate new regulators of these pathways.

Methods

Materials and methods are provided in *SI Appendix, Materials and Methods*. These include general materials and methods, synthetic procedures, cell culture, lentivirus production, CRISPRi screen, IMPACT labeling with HPLC or flow cytometry analysis, butanol transphosphatidylation assay, 3-(4,5-dimethylthiazol-2-yl)-2,5-diphenyltetrazolium bromide (MTT) assay, Western blot, qPCR, and statistical methods.

Data Availability. All study data are included in the article and/or *SI Appendix*.

ACKNOWLEDGMENTS. J.M.B. acknowledges support from the NSF (CAREER CHE-1749919), the Arnold and Mabel Beckman Foundation (Beckman Young Investigator Award), and the Alfred P. Sloan Foundation (Sloan Research Fellowship). T.W.B. was supported by an NSF graduate research fellowship (DGE-1650441), S.H. was supported by a Cornell Fellowship and the NIH (T32GM138826), and R.T. was supported by Honjo International, Funai Overseas, and Cornell Fellowships. FACS was performed at the Cornell Institute of Biotechnology Flow Cytometry Facility. We thank Martin Kampmann (University of California, San Francisco) for the generous gift of K562-dCas9-KRAB cells and helpful advice; the Emr, Fromme, and Hu laboratories (Cornell) for use of equipment; and members of the Baskin laboratory for helpful discussions.

1. C. H. Heldin, B. Lu, R. Evans, J. S. Gutkind, Signals and receptors. *Cold Spring Harb. Perspect. Biol.* **8**, a005900 (2016).
2. A. C. Newton, M. D. Bootman, J. D. Scott, Second messengers. *Cold Spring Harb. Perspect. Biol.* **8**, a00592 (2016).
3. R. K. Nelson, M. A. Frohman, Physiological and pathophysiological roles for phospholipase D. *J. Lipid Res.* **56**, 2229–2237 (2015).
4. P. E. Selvy, R. R. Lavieri, C. W. Lindsley, H. A. Brown, Phospholipase D: Enzymology, functionality, and chemical modulation. *Chem. Rev.* **111**, 6064–6119 (2011).
5. M. A. Frohman, The phospholipase D superfamily as therapeutic targets. *Trends Pharmacol. Sci.* **36**, 137–144 (2015).
6. H. A. Brown, P. G. Thomas, C. W. Lindsley, Targeting phospholipase D in cancer, infection and neurodegenerative disorders. *Nat. Rev. Drug Discov.* **16**, 351–367 (2017).
7. L. Santa-Marinha *et al.*, Phospholipase D1 ablation disrupts mouse longitudinal hippocampal axis organization and functioning. *Cell Rep.* **30**, 4197–4208.e6 (2020).
8. O. Shalem *et al.*, Genome-scale CRISPR-Cas9 knockout screening in human cells. *Science* **343**, 84–87 (2014).
9. L. A. Gilbert *et al.*, Genome-scale CRISPR-mediated control of gene repression and activation. *Cell* **159**, 647–661 (2014).
10. T. Wang, J. J. Wei, D. M. Sabatini, E. S. Lander, Genetic screens in human cells using the CRISPR-Cas9 system. *Science* **343**, 80–84 (2014).
11. L. A. Gilbert *et al.*, CRISPR-mediated modular RNA-guided regulation of transcription in eukaryotes. *Cell* **154**, 442–451 (2013).
12. G. V. Pusapati *et al.*, CRISPR screens uncover genes that regulate target cell sensitivity to the morphogen sonic hedgehog. *Dev. Cell* **44**, 113–129.e8 (2018).
13. O. Parnas *et al.*, A genome-wide CRISPR screen in primary immune cells to dissect regulatory networks. *Cell* **162**, 675–686 (2015).
14. C. G. Parker, M. R. Pratt, Click chemistry in proteomic investigations. *Cell* **180**, 605–632 (2020).
15. E. M. Sletten, C. R. Bertozzi, Bioorthogonal chemistry: Fishing for selectivity in a sea of functionality. *Angew. Chem. Int. Ed. Engl.* **48**, 6974–6998 (2009).
16. H. C. Hang, J. P. Wilson, G. Charron, Bioorthogonal chemical reporters for analyzing protein lipidation and lipid trafficking. *Acc. Chem. Res.* **44**, 699–708 (2011).
17. J. Du *et al.*, Metabolic glycoengineering: Sialic acid and beyond. *Glycobiology* **19**, 1382–1401 (2009).
18. B. F. Cravatt, A. T. Wright, J. W. Kozarich, Activity-based protein profiling: From enzyme chemistry to proteomic chemistry. *Annu. Rev. Biochem.* **77**, 383–414 (2008).
19. K. J. Bruemmer, S. W. M. Crossley, C. J. Chang, Activity-based sensing: A synthetic methods approach for selective molecular imaging and beyond. *Angew. Chem. Int. Ed. Engl.* **59**, 13734–13762 (2020).
20. M. F. Debets *et al.*, Metabolic precision labeling enables selective probing of O-linked *N*-acetylgalactosamine glycosylation. *Proc. Natl. Acad. Sci. U.S.A.* **117**, 25293–25301 (2020).
21. G. M. Lenk *et al.*, CRISPR knockout screen implicates three genes in lysosome function. *Sci. Rep.* **9**, 9609 (2019).
22. J. Y. Cao *et al.*, A genome-wide haploid genetic screen identifies regulators of glutathione abundance and ferroptosis sensitivity. *Cell Rep.* **26**, 1544–1556.e8 (2019).
23. T. W. Bumpus, J. M. Baskin, Clickable substrate mimics enable imaging of phospholipase D activity. *ACS Cent. Sci.* **3**, 1070–1077 (2017).
24. T. W. Bumpus, F. J. Liang, J. M. Baskin, Ex uno plura: Differential labeling of phospholipid biosynthetic pathways with a single bioorthogonal alcohol. *Biochemistry* **57**, 226–230 (2018).
25. T. W. Bumpus, D. Liang, J. M. Baskin, IMPACT: Imaging phospholipase d activity with clickable alcohols via transphosphatidylation. *Methods Enzymol.* **641**, 75–94 (2020).
26. T. W. Bumpus, J. M. Baskin, A chemoenzymatic strategy for imaging cellular phosphatidic acid synthesis. *Angew. Chem. Int. Ed. Engl.* **55**, 13155–13158 (2016).
27. D. Liang *et al.*, A real-time, click chemistry imaging approach reveals stimulus-specific subcellular locations of phospholipase D activity. *Proc. Natl. Acad. Sci. U.S.A.* **116**, 15453–15462 (2019).
28. A. C. Newton, Protein kinase C: Structural and spatial regulation by phosphorylation, cofactors, and macromolecular interactions. *Chem. Rev.* **101**, 2353–2364 (2001).
29. M. Kampmann, CRISPRi and CRISPRa screens in mammalian cells for precision biology and medicine. *ACS Chem. Biol.* **13**, 406–416 (2018).
30. M. A. Horlbeck *et al.*, Compact and highly active next-generation libraries for CRISPR-mediated gene repression and activation. *eLife* **5**, e19760 (2016).
31. S. H. Alamudi *et al.*, Development of background-free tame fluorescent probes for intracellular live cell imaging. *Nat. Commun.* **7**, 11964 (2016).
32. T. Nagy, M. Kampmann, CRISPulator: A discrete simulation tool for pooled genetic screens. *BMC Bioinformatics* **18**, 347 (2017).
33. G. Du *et al.*, Dual requirement for rho and protein kinase C in direct activation of phospholipase D1 through G protein-coupled receptor signaling. *Mol. Biol. Cell* **11**, 4359–4368 (2000).
34. M. J. Hart *et al.*, Direct stimulation of the guanine nucleotide exchange activity of p115 RhoGEF by Galpha13. *Science* **280**, 2112–2114 (1998).
35. T. Kozasa *et al.*, p115 RhoGEF, a GTPase activating protein for Galpha12 and Galpha13. *Science* **280**, 2109–2111 (1998).
36. M. J. Hart *et al.*, Identification of a novel guanine nucleotide exchange factor for the Rho GTPase. *J. Biol. Chem.* **271**, 25452–25458 (1996).
37. J. B. Li *et al.*, Comparative genomics identifies a flagellar and basal body proteome that includes the BBS5 human disease gene. *Cell* **117**, 541–552 (2004).
38. M. Gegg *et al.*, Flattop regulates basal body docking and positioning in mono- and multiciliated cells. *eLife* **3**, e03842 (2014).
39. E. Efimenko *et al.*, Caenorhabditis elegans DYF-2, an orthologue of human WDR19, is a component of the intraflagellar transport machinery in sensory cilia. *Mol. Biol. Cell* **17**, 4801–4811 (2006).
40. K. F. Lechtreck *et al.*, Cycling of the signaling protein phospholipase D through cilia requires the BBSome only for the export phase. *J. Cell Biol.* **201**, 249–261 (2013).
41. P. Liu, K. F. Lechtreck, The Bardet-Biedl syndrome protein complex is an adapter expanding the cargo range of intraflagellar transport trains for ciliary export. *Proc. Natl. Acad. Sci. U.S.A.* **115**, E934–E943 (2018).
42. Y.-X. Liu *et al.*, Bardet-Biedl syndrome 3 protein promotes ciliary exit of the signaling protein phospholipase D via the BBSome. *eLife* **10**, e59119 (2021).
43. A. C. Newton, Protein kinase C: Perfectly balanced. *Crit. Rev. Biochem. Mol. Biol.* **53**, 208–230 (2018).
44. E. Beurel, S. F. Grieco, R. S. Jope, Glycogen synthase kinase-3 (GSK3): Regulation, actions, and diseases. *Pharmacol. Ther.* **148**, 114–131 (2015).
45. M. Zhong *et al.*, Phospholipase D prevents apoptosis in v-Src-transformed rat fibroblasts and MDA-MB-231 breast cancer cells. *Biochem. Biophys. Res. Commun.* **302**, 615–619 (2003).
46. T. A. Engler *et al.*, Substituted 3-imidazo[1,2-a]pyridin-3-yl- 4-(1,2,3,4-tetrahydro-[1,4]diazepino-[6,7,1-hi]indol-7-yl)pyrrole-2,5-diones as highly selective and potent inhibitors of glycogen synthase kinase-3. *J. Med. Chem.* **47**, 3934–3937 (2004).

47. H. A. Brown, L. G. Henage, A. M. Preininger, Y. Xiang, J. H. Exton, Biochemical analysis of phospholipase D. *Methods Enzymol.* **434**, 49–87 (2007).
48. F. F. Wagner *et al.*, Exploiting an Asp-Glu "switch" in glycogen synthase kinase 3 to design paralog-selective inhibitors for use in acute myeloid leukemia. *Sci. Transl. Med.* **10**, eaam8460 (2018).
49. D. Wu, W. Pan, GSK3: A multifaceted kinase in Wnt signaling. *Trends Biochem. Sci.* **35**, 161–168 (2010).
50. R. Nusse, H. Clevers, Wnt/β-catenin signaling, disease, and emerging therapeutic modalities. *Cell* **169**, 985–999 (2017).
51. D. W. Kang, S. Min, Positive feedback regulation between phospholipase D and Wnt signaling promotes Wnt-driven anchorage-independent growth of colorectal cancer cells. *PLoS One* **5**, e12109 (2010).
52. T. Hu, J. H. Exton, Mechanisms of regulation of phospholipase D1 by protein kinase Calpha. *J. Biol. Chem.* **278**, 2348–2355 (2003).
53. S. M. Hammond *et al.*, Characterization of two alternately spliced forms of phospholipase D1. Activation of the purified enzymes by phosphatidylinositol 4,5-bisphosphate, ADP-ribosylation factor, and Rho family monomeric GTP-binding proteins and protein kinase C-alpha. *J. Biol. Chem.* **272**, 3860–3868 (1997).
54. S. M. Hammond *et al.*, Human ADP-ribosylation factor-activated phosphatidylcholine-specific phospholipase D defines a new and highly conserved gene family. *J. Biol. Chem.* **270**, 29640–29643 (1995).
55. P. M. Steed, K. L. Clark, W. C. Boyar, D. J. Lasala, Characterization of human PLD2 and the analysis of PLD isoform splice variants. *FASEB J.* **12**, 1309–1317 (1998).
56. S. F. Moore *et al.*, Dual regulation of glycogen synthase kinase 3 (GSK3)α/β by protein kinase C (PKC)α and Akt promotes thrombin-mediated integrin αIIbβ3 activation and granule secretion in platelets. *J. Biol. Chem.* **288**, 3918–3928 (2013).
57. J. S. Chen, J. H. Exton, Regulation of phospholipase D2 activity by protein kinase C α. *J. Biol. Chem.* **279**, 22076–22083 (2004).
58. T. K. Harden, G. L. Waldo, S. N. Hicks, J. Sondek, Mechanism of activation and inactivation of Gq/phospholipase C-β signaling nodes. *Chem. Rev.* **111**, 6120–6129 (2011).
59. P. Patel, J. R. Woodgett, Glycogen synthase kinase 3: A kinase for all pathways? *Curr. Top. Dev. Biol.* **123**, 277–302 (2017).
60. L. He *et al.*, Regulation of GSK3 cellular location by FRAT modulates mTORC1-dependent cell growth and sensitivity to rapamycin. *Proc. Natl. Acad. Sci. U.S.A.* **116**, 19523–19529 (2019).
61. T. W. Bumpus, J. M. Baskin, Greasing the wheels of lipid biology with chemical tools. *Trends Biochem. Sci.* **43**, 970–983 (2018).